


Effect of Alloy Chemistry and Growth Rate on the Unidirectional Solidification behaviour of Single Crystal Superalloys

N. Hazari¹  · D. Chatterjee¹ · Daisy Priya Tigga¹ · N. Das¹

Received: 11 July 2015 / Accepted: 8 September 2015 / Published online: 13 October 2015
© The Indian Institute of Metals - IIM 2015

Abstract The addition of Re to Ni-based cast superalloys significantly changes the solidification behaviour and thereby improves the creep strength and resistance to high temperature corrosion and oxidation in both columnar grained and single crystal blades. This is because the partitioning behaviour of Re is different from that of other alloying additions in nickel based superalloys. Re containing alloys in the present study solidifies as dendrites of γ -phase together with inter dendritic eutectic of γ - γ' . It has been observed that the growth rate, apart from affecting the solidification structure influences the solid-state transformation of γ - γ' and thus changes the γ - γ' distribution and morphology.

Keywords Investment casting · Directional solidification · Single crystal · Dendritic growth

1 Introduction

Turbine engine manufacturers have achieved a remarkable improvement in the fuel efficiency and thrust of gas turbine engines primarily because of the development of superior nickel based superalloys. The innovations in component processing to produce directionally solidified columnar grained as well as single crystal castings incorporating intricate cooling channels together with the design of new superalloys, made it possible to achieve high service

temperatures together with component durability and engine life.

The addition of Re and Ru to nickel-based superalloys results in improved creep strength and resistance to high temperature corrosion and oxidation in both directionally solidified columnar-grained and single crystal blades and vanes [1, 2]. The partitioning behaviour of Re is different from other alloying additions in nickel based superalloys [3]. Re addition strongly increases the eutectic content and the tendency for micro segregation [4]. The solidification characteristics of Re containing nickel based superalloys depict several beneficial effects. This large, heavy element partitions preferentially to the γ matrix providing strengthening through solid solution hardening at high temperatures. It also increases the melting temperature of the alloy. In addition to solid-solution hardening to the matrix phase, Re increases the γ/γ' misfit and imparts additional strengthening [5, 6]. Re increases the liquidus temperature and decreases the γ' -solvus. Also, Re addition strongly increases the eutectic content and the tendency for micro segregation [4].

Three multi component single crystal alloys containing Re in the range of 1.5–6 wt% developed at Defence Metallurgical Research Laboratory (DMRL), Hyderabad, have been chosen for the present study. These are characterized for the influence of Re on as-cast microstructure, and segregation behaviour. These alloys have been unidirectionally solidified under different growth rates while keeping the temperature gradient constant.

2 Materials and Experimental Procedure

The alloys used in the present study were melted in a vacuum induction melting furnace in the form of 5 kg ingot; the chemical compositions are shown in Table 1.

✉ N. Hazari
n_hazari@yahoo.com

¹ Enabling Technology Centre for Investment Casting,
Defence Metallurgical Research Laboratory, Hyderabad
500058, India

Table 1 Compositions (wt%) of investigated alloys obtained by chemical analysis

Alloys	Ni	Cr	Co	Mo	W	Re	Ta	Al	Ti	Hf	O (ppm)	N (ppm)
DMSX-1 (nominal)	61.7	7.9	6.7	1.0	7.0	1.5	7.7	5.5	1.0	–	<10	<10
Analyzed	61.5	7.6	6.5	0.8	6.8	1.2	7.5	5.3	0.9	–	<10	<10
DMSX-4 (nominal)	66.9	6.2	–	2.3	4.4	6.0	8.5	5.6	–	0.1	<10	<10
Analyzed	66.6	6.0	–	2.1	4.3	5.9	8.4	5.4	–	0.1	<10	<10
DMSX-6 (nominal)	62.6	5.9	6.7	0.9	5.9	3.6	7.9	5.3	1.0	0.1	<10	<10
Analyzed	62.5	5.7	6.5	0.8	5.4	3.5	7.6	5.2	0.8	0.08	<10	<10

The ingots were subsequently re-melted and cast as rods by investment casting technique. These rods were again re-melted in recrystallized alumina tube and directionally solidified into rods of 12 mm diameter, using a vacuum directional solidification furnace (Model-3026-1, Geophysics Corporation of America, MA, USA) at different withdrawal rate. The first 20 mm was withdrawn at a speed of 5 cm/h, next 30 mm with a speed of 20 cm/h, next 30 mm with 40 cm/h and the rest with 60 cm/h. During withdrawal, the furnace temperature was maintained at 1500 °C and the average temperature gradient was measured as 50 °C/cm.

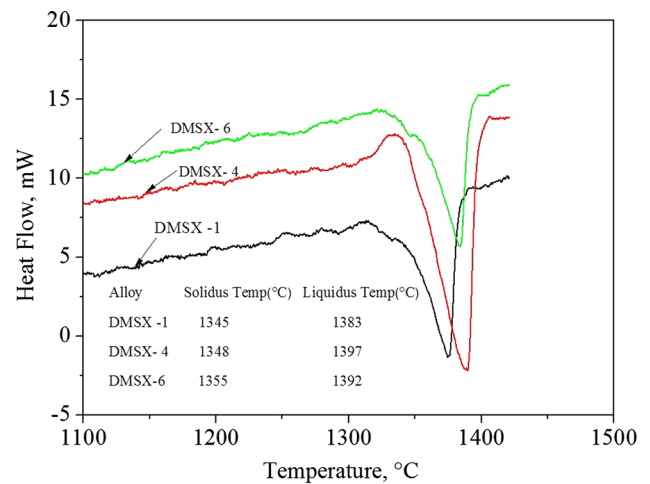
After solidification, the rods were chemically etched to identify the transition lines of different withdrawal rate. The rods were cut normal to the growth direction and at 10 mm above each transition line. Thermal analysis was carried out using differential scanning calorimeter (DSC) for all three as cast alloys. Microstructural characterization of specimens were carried out using optical microscope (OM), scanning electron microscope (SEM) and electron probe micro analyzer (EPMA).

3 Results and Discussion

The DSC plots for all the three alloys are shown in Fig. 1. The plots suggest that the liquidus temperature increases with Re content in the alloys. Figure 2 shows as cast micro structures of all three alloys with two basic constituents: (1) Primary dendrite and (2) interdendritic phase aggregate solidified at minimum and maximum withdrawal rates. The primary dendrites have four fold secondary arms to one another. Tertiary branchings are also observed for some of the conditions (Fig. 2d).

Figure 3 shows the SEM images of primary dendrites at minimum and maximum withdrawal rates showing a two phase microstructures of γ and γ' .

Figure 4 shows the average primary dendrite arms spacing (PDAS) of all the alloys with Re content at different withdrawal rate. The dendrites become finer with Re as well as with increasing withdrawal rates. This implies that the coring effect is more pronounced with Re content.

**Fig. 1** DSC Plots for all three alloys

The finer dendrites are expected with the increase of withdrawal rate.

Detailed EPMA analyses reveals that concentrations of Co, W and Re are high in dendrite as compared to interdendritic regions whereas other elements like Cr, Ta and Ti are enriched more in interdendritic regions. Such behaviour for rhenium is shown in Fig. 5. It is obvious that rhenium partitions to dendritic region rather than the interdendritic region.

Figure 6 shows that the volume fraction of interdendritic region increases with the increase in withdrawal rate for all the alloys. This effect can be directly correlated with higher withdrawal rates leading to the increase in cooling rate at a constant temperature gradient. As the cooling rate increases, there is less time for dendrite to grow. As a result, there is more liquid at the end of solidification. The liquid solidifies eutectically giving rise to smaller volume fraction of dendrite. Similarly, it is seen that with increasing rhenium content, the volume fraction of interdendritic region goes through a maximum for all the withdrawal rates (Fig. 7) [11].

Figure 8 shows a map presenting the different solidification morphologies obtained under various conditions of growth rate and temperature gradient for nickel based

Fig. 2 Backscattered electron micrographs in as polished condition of all the alloys directionally solidified at minimum and maximum withdrawal rates. **a** DMSX-1 alloy, $R = 14 \mu\text{m/s}$; **b** DMSX-1, $R = 165 \mu\text{m/s}$; **c** DMSX-6, $R = 14 \mu\text{m/s}$; **d** DMSX-6, $R = 165 \mu\text{m/s}$; **e** DMSX-4, $R = 14 \mu\text{m/s}$; **f** DMSX-4, $R = 165 \mu\text{m/s}$

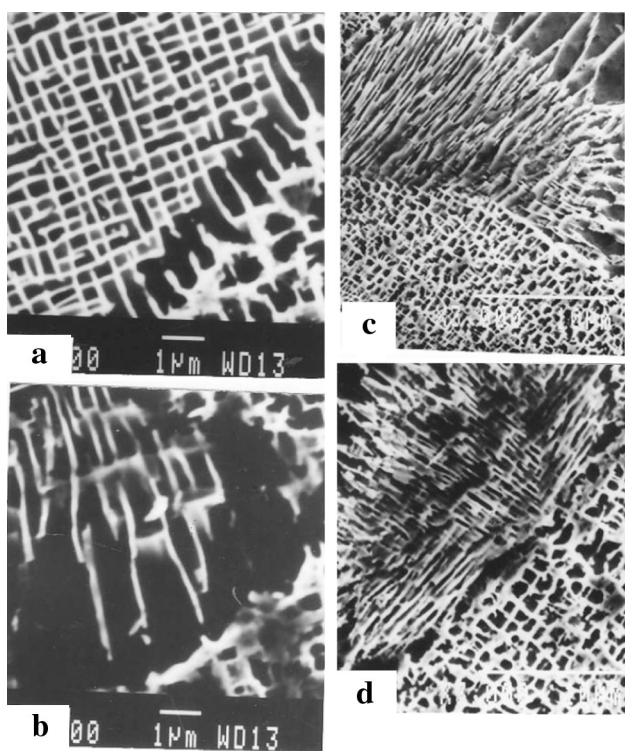
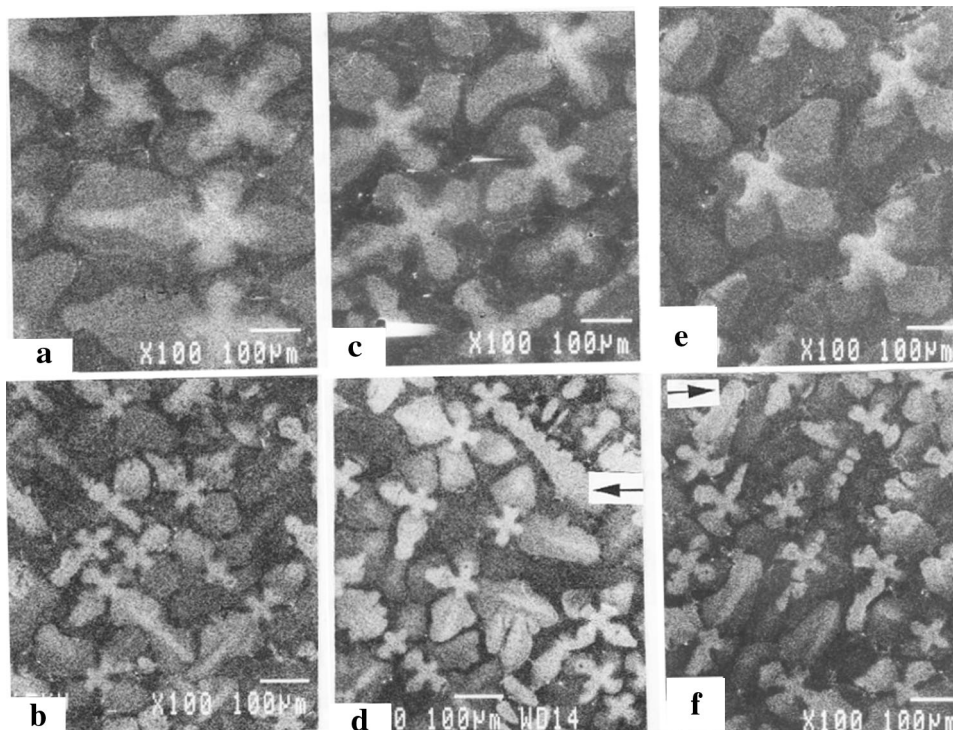


Fig. 3 Secondary electron images of interdendritic regions of selected alloys at the minimum and maximum withdrawal rates showing the eutectic aggregate of γ and γ' . **a** DMSX-1 alloy, $R = 14 \mu\text{m/s}$; **b** DMSX-1, $R = 165 \mu\text{m/s}$; **c** DMSX-4, $R = 14 \mu\text{m/s}$; **d** DMSX-4, $R = 165 \mu\text{m/s}$

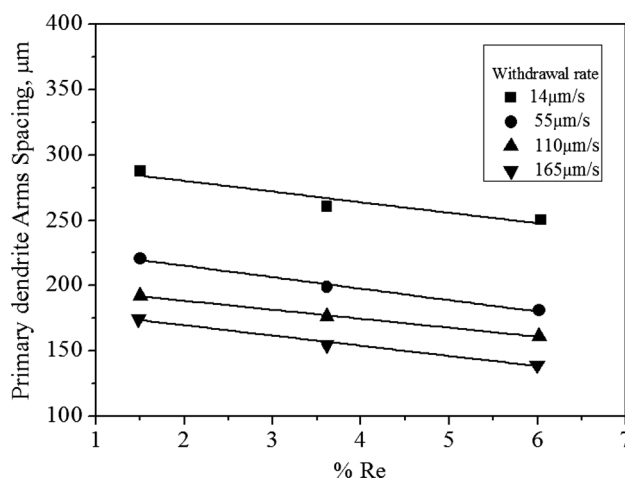


Fig. 4 PDAS as a function of rhenium content at different withdrawal rates

superalloys [7]. The data from the present investigation are also superimposed. These are towards upper bound of dendritic region in the microstructural map. The specimen which are in the equiaxed region of the map still show dendritic features. The inconsistency may be due to the inaccurate measurement of temperature gradient, G which needs to be measured using more elaborate and sophisticated technique, as suggested by Pollock et al. [10].

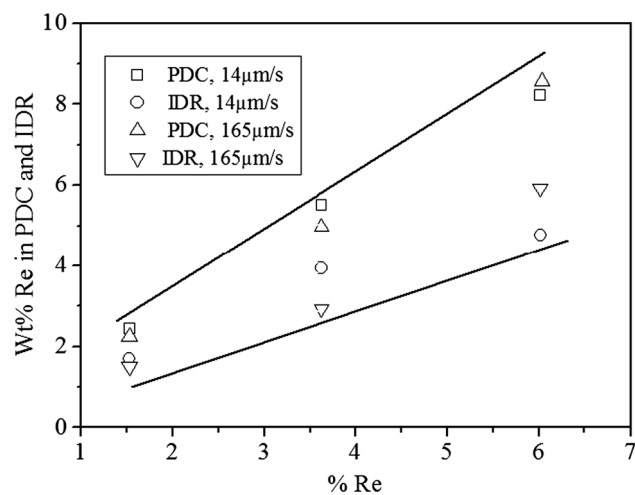


Fig. 5 Variation in rhenium in the primary dendrite centre (PDC) and interdendritic region (IDR) with Re at different withdrawal rates

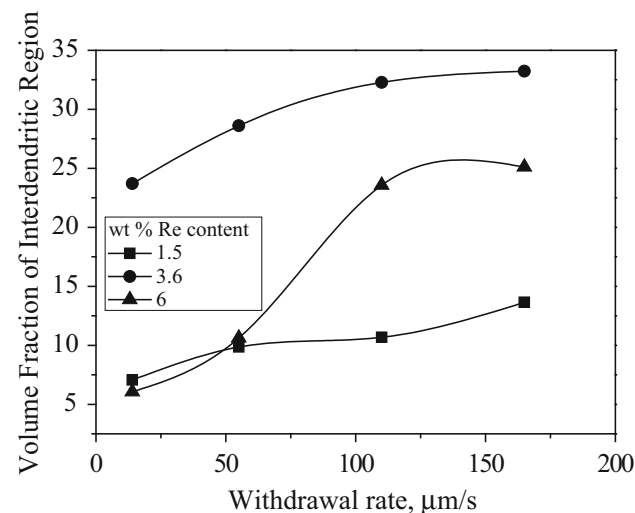


Fig. 6 Vol. fraction of interdendritic region as a function of withdrawal rate

From Fig. 4, it can be observed that the PDAS decreases with withdrawal rate. The variation of PDAS as a function of $R^{-0.25} G^{-0.50}$ for different alloys is shown in Fig. 9. It can be seen from this figure that PDAS is linear function of $R^{-0.25} G^{-0.50}$. Thus data for the present alloys system vindicate the validity of equation $\lambda_1 = R^{-0.25} G^{-0.50}$. A log–log plot of PDAS versus withdrawal rate for all the three alloys is shown in Fig. 10.

The trend is linear indicating validity of the equation. However, the exponent is 0.2 which is lower than the theoretical value (0.25) but higher than (0.16) reported for Ni_3Al [7].

In order to obtain a further insight into the growth behaviour, the present results are compared with the predicted results by the models proposed by Kurz and Fisher

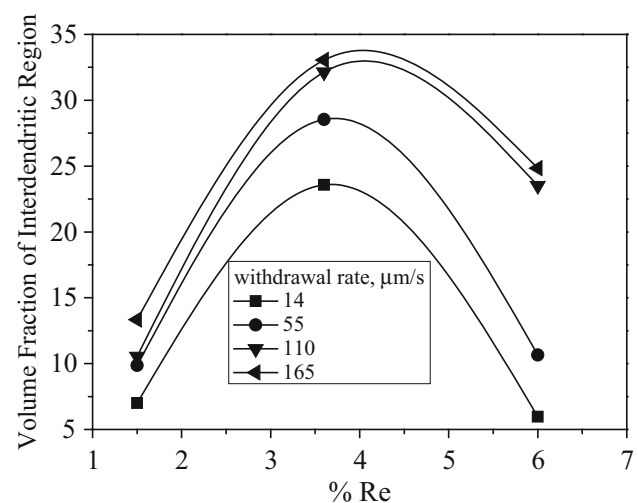


Fig. 7 Vol. fraction of interdendritic region as a function of rhenium content

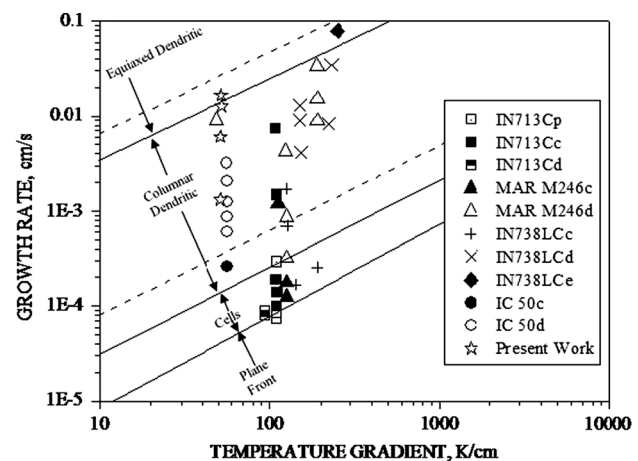


Fig. 8 Summary plot showing the different solidification morphologies obtained under various combinations of withdrawal rate and temperature. Also superimposed are the results of the present work [12]

and Hunt [8, 9]. This comparison was made after making certain assumptions in the physical properties of the alloys used in the present study; i.e. the physical property data are taken from those of Ni_3Al intermetallic [7]. The data of the present alloy set are bound very well by the theoretical lines (Fig. 11). This indicates that solidification mechanism for the rhenium containing alloys in the present study is intermediate between the mechanism proposed by Kurz and Fisher [8] and Hunt [9].

It is interesting to observe that the volume fraction and size of γ' decreases with withdrawal rate (Figs. 12, 13). This implies that while the growth rate is expected to affect the solidified microstructures, it indirectly influences the solid state transformation by reducing the size and volume fraction of γ' . As the growth rate increases, the portion of

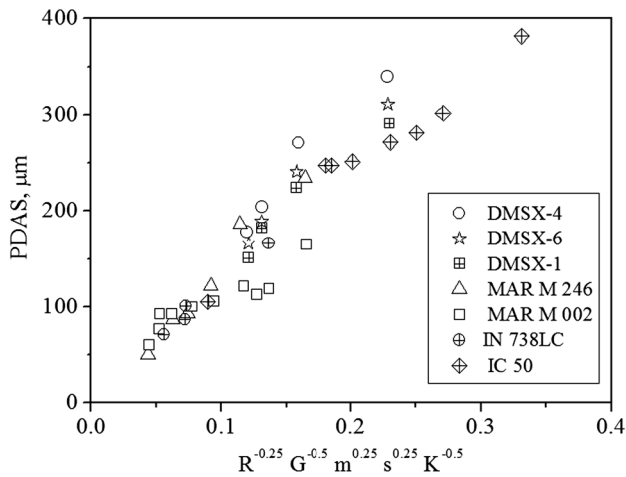


Fig. 9 Variation in the value of PDAS as a function of $R^{-0.25} G^{-0.50}$ of different Ni-based superalloys along with the present work [7]

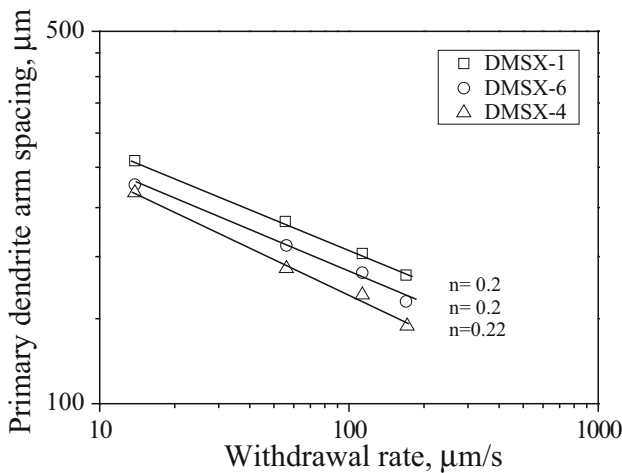


Fig. 10 Log–log plot of PDAS versus withdrawal rate [7]

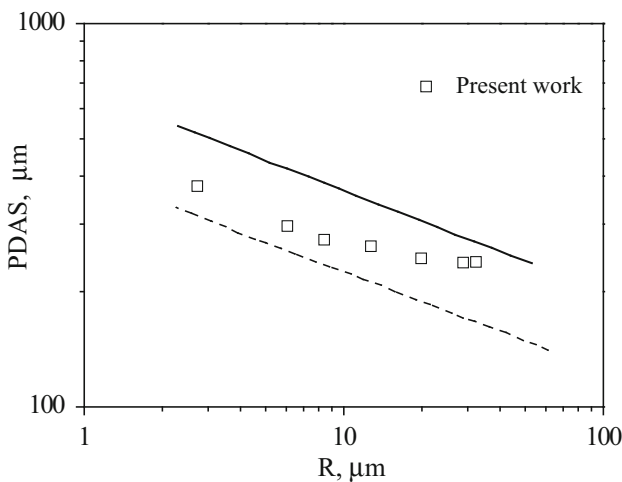


Fig. 11 PDAS as a function of withdrawal rate. The *solid lines* correspond to theoretical predictions derived from Kurz and Fischer [8] and Hunt [9]

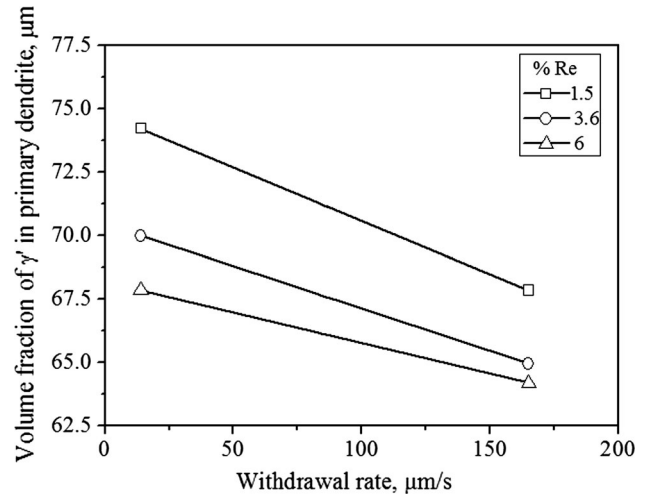


Fig. 12 Volume fraction of γ' in primary dendrite as a function of withdrawal rate

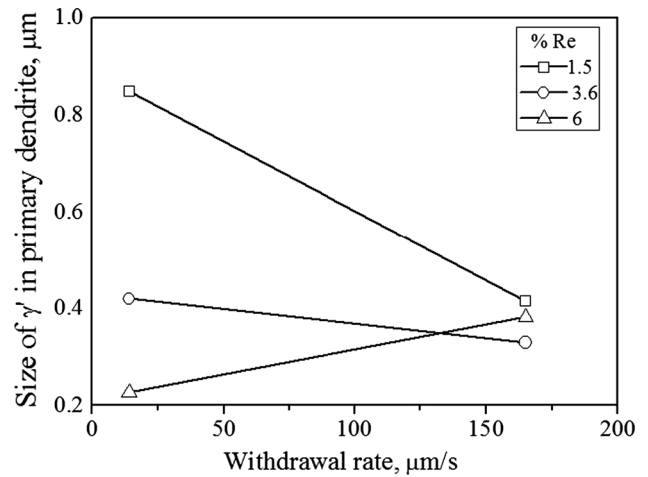


Fig. 13 Size of γ' in primary dendrite as a function of withdrawal rate

the rod which has solidified, moves away from hot zone and thus loses heat rapidly.

Because of this, as the temperature comes down through the γ - γ' solvus, the cooling rate increases. This results in growing more number of nuclei of γ' within γ and also less time for the γ' precipitate to grow. As cooling rate is the product of growth rate and temperature gradient, therefore with increasing growth rate, cooling rate increases. Consequently, this increases the under cooling for γ' that is to be precipitated. This increases nucleation rate and decreases growth of precipitate.

4 Conclusion

1. PDAS decreases with withdrawal rate following the classical theoretical models for conventional solidification of binary alloys.

2. The growth rate reduces the volume fraction and size of γ' in primary dendrites.

Acknowledgment The present study is a part of the project (DMR-294) sanctioned by DRDO. Authors also wish to thank Director, DMRL for his encouragement and support.

References

1. Donachie M J, and Donachie S J, *Superalloys: A Technical Guide*, 2nd ed., ASM International (2002).
2. Ko H S, Paik K W, Park L J, Kim Y G, and Tunderman J H, *J Mater Sci* **33** (1998) 3361.
3. Geddes B, Leon H, and Huang X, *Superalloys: Alloying and Performance*, ASM International (2010).
4. Wolmer S, and Glatzel U, *Mater Sci Eng A*, **319–321** (2001).
5. Piearcy B J, and Versnyder F L, *J Aircr* **3** (1996) 390.
6. Heckl A, Rettig R, and Singer R F, *Metall Mater Trans A* (2009).
7. Kim H K, Earthman J C, and Lavernia E J, *Acta Metall Mater* **40** (1992).
8. Kurz W, and Fisher D J, *Acta Metall* **29** (1981) 11.
9. Hunt J D, and Burden M H, *J Cryst Growth* **22** (1974) 99.
10. Pollock T M, and Murphy W H, *Metall Mater Trans A* **27A** (1996).
11. Copley S M, and Kear B H, *Trans Met Soc AIME* **239** (1967).
12. Quested P N, and Mclean M, *Mater Sci Eng* **65** (1984).